Science Translational Medicine
AAAS

Supplementary Materials for

Gene therapy knockdown of Hippo signaling induces cardiomyocyte renewal in pigs after myocardial infarction

Shijie Liu *et al.*

Corresponding author: James F. Martin, jfmartin@bcm.edu

Sci. Transl. Med. **13**, eabd6892 (2021)
DOI: 10.1126/scitranslmed.abd6892

The PDF file includes:

Figs. S1 to S11
Tables S1 to S6
Legends for movies S1 to S6

Other Supplementary Material for this manuscript includes the following:

Data file S1
Movies S1 to S6

Supplementary movies S1-S6

Echocardiograms show AAV9-GFP (P-1894) and AAV9-*Sav*-shRNA-injected hearts (P-2022, high-dose) at day 0 (baseline movie S1, S2), day 14 (2 weeks after myocardial infarction, movie S3, S4), and day 104 (3 months after viral injection, movie S5, S6).

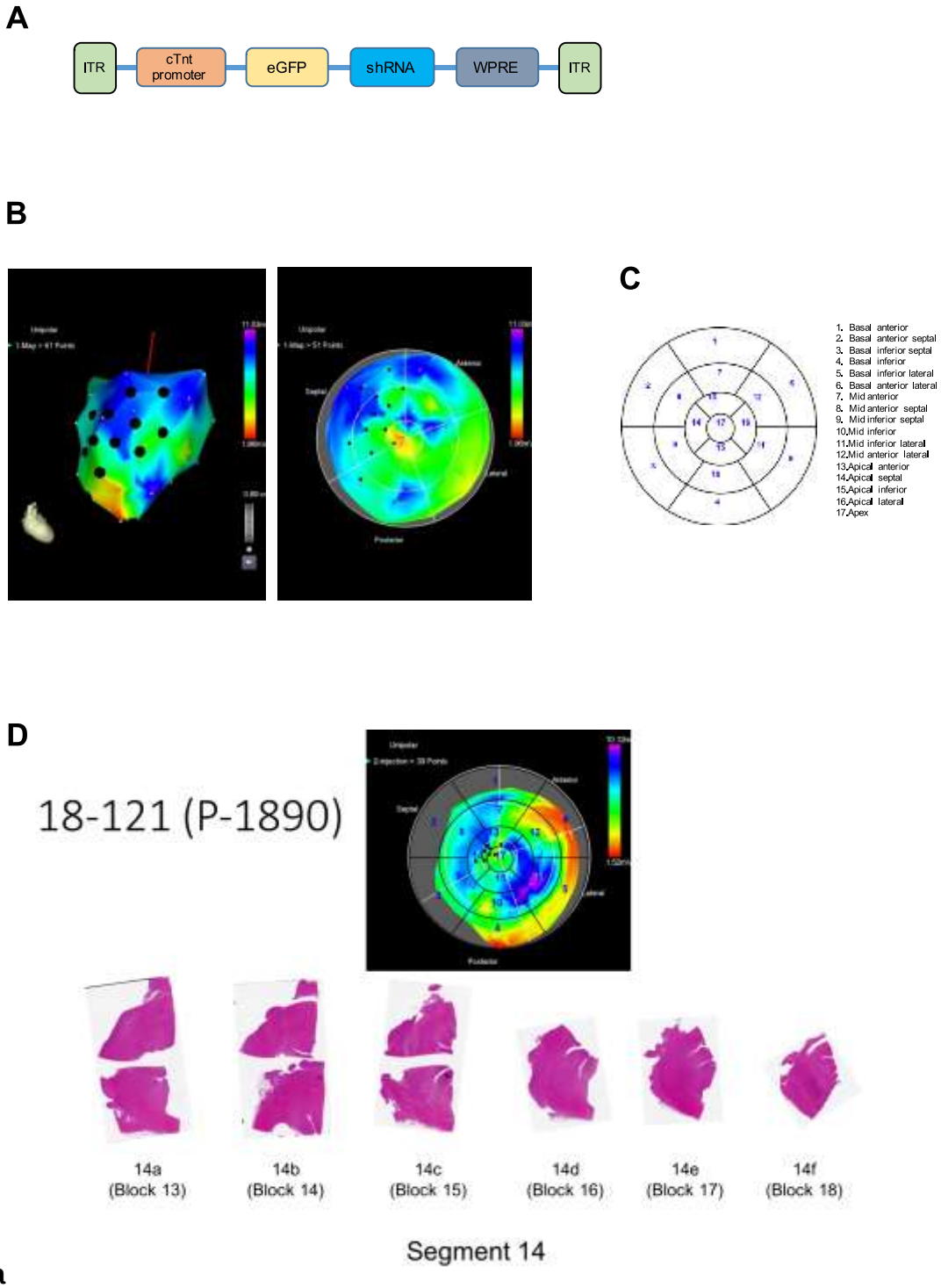

Fig. S1 AAV9 virus administration and pig sample processing. (**A**) Schematic of the AAV9-*Sav*-shRNA vector. (**B**) Representative images from pig P-1922 showing the virus

injection sites (black dots) on the electromechanical mapping (EMM) system. (**C**) Annotation of heart segments. (**D**) EMM map for pig P-1890. Segments were processed for histologic analysis; based on hematoxylin and eosin staining, segments near the injection sites were selected for immunofluorescence staining.

Liu et al. Fig. s2

A

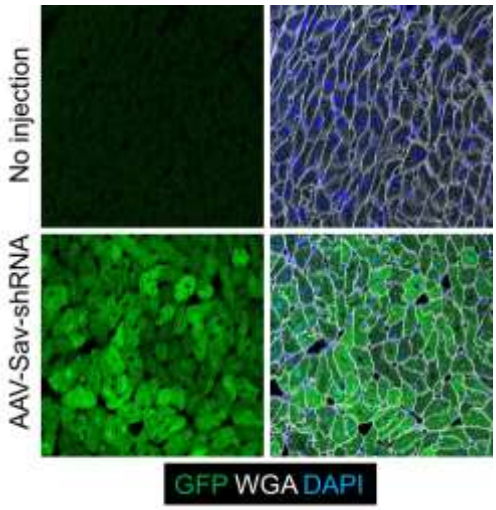

B

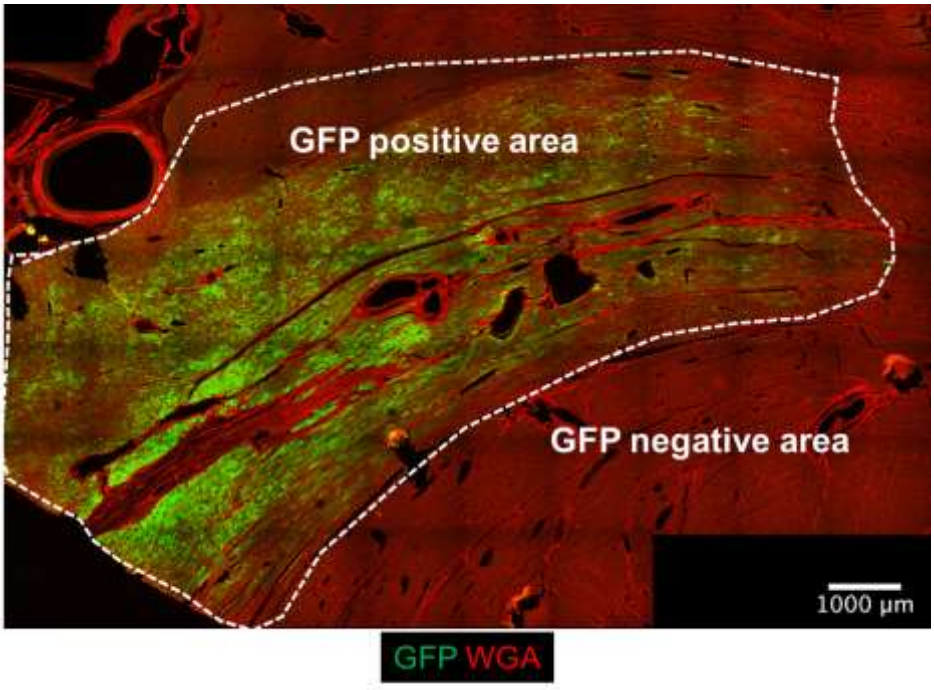

Fig. S2 IF staining revealing GFP-positive areas. (**A, B**) Three months after viral injection, sections were stained with a GFP antibody.

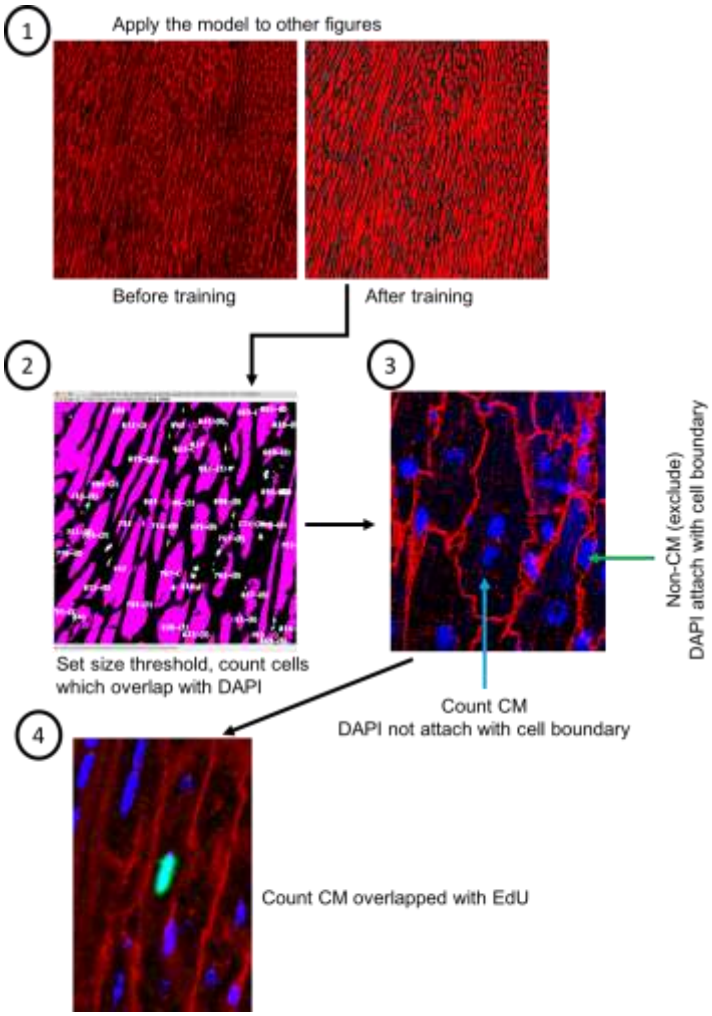

Fig. S3 Pipeline of machine learning. 1. The WAG channel of tiled images were analyzed by Fiji to identify the cell boundary and then used for segmentation with machine learning. 2. Segmentations were counted, and size was measured. Segmentation area greater than 100 pixels were identified as the CMs. 3. Further filters to identify CMs. Segmentations with DAPI, which were distinct from the cell boundary, were counted as the CMs. 4. EdU channel identification of the EdU positive CMs.

Liu et al. Fig. s4

A

P-1946	EF	LVEDV	LVESV	SV
Day0	60%	59ml	23ml	36ml
Day14	30%	65ml	46ml	23ml

B

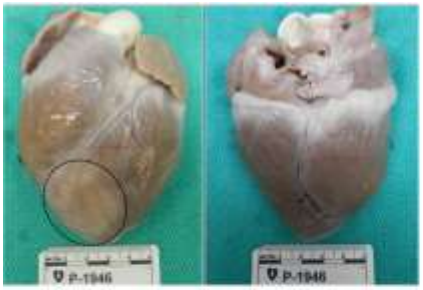

C

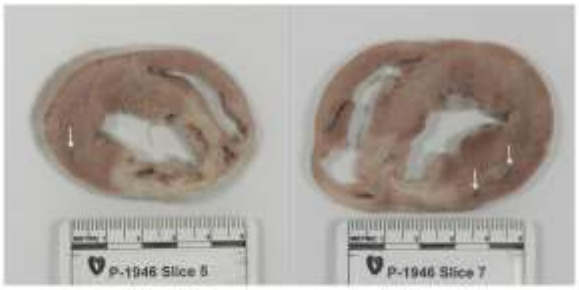

D

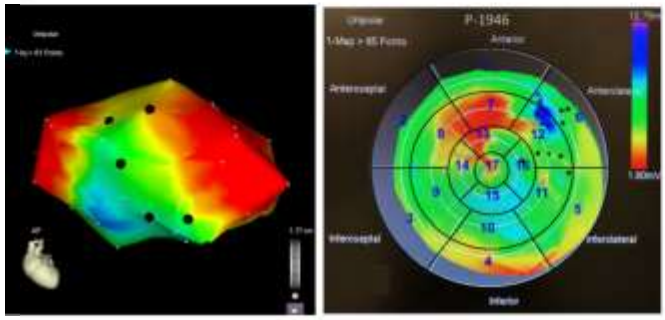

Fig. S4 Pig model of MI. (**A**) Echocardiographic results from pig P-1946 showing that heart function decreased at 14 days after MI. (**B**) Gross heart images show transmural scar in the anterior area near the apex. (**C**) Heart slices show infarct tissue. White arrows indicate focal hemorrhage suggestive of NOGA injection sites. (**D**) Three-dimensional (left) and two-dimensional (right) EMM maps show the injection sites. The area highlighted red at the apex is infarct tissue. The area highlighted green or blue is normal tissue. White dots indicate the probed sites for building the three-dimensional heart model. Black dots indicate virus injection sites.

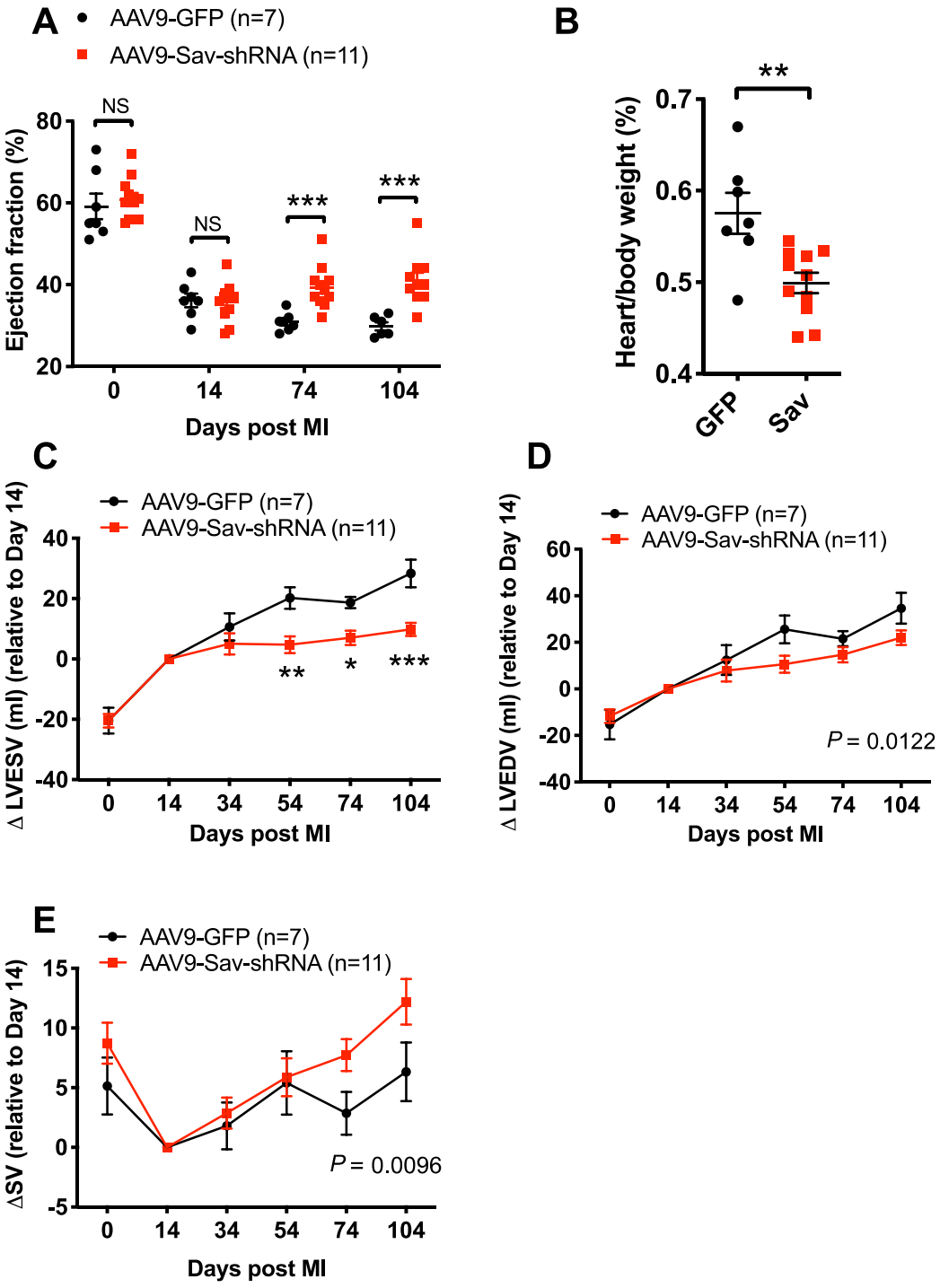

Fig. S5 Heart regeneration in *Sav* knockdown pigs. Echocardiography reveals improved contractile function in hearts injected with AAV9-*Sav*-shRNA than in hearts

injected with AAV9-GFP at different time points. Day 0 indicates the day of myocardial infarction, and day 14 indicates the day of virus injection. (**A**) Ejection fraction at different time points in pigs injected with AAV9-GFP (n=7) or AAV9-*Sav*-shRNA (n=11: 8 pigs received a regular dose, 3 pigs received a high-dose). (**B**) Heart weight/body weight for pigs at 90 days after virus injection. (GFP, AAV9-GFP, n=7; Sav, AAV9-Sav-shRNA, low and high-dose combined, n=11). (**C**) Change (relative to day 14) in left ventricular end-systolic volume (LVESV). (**D**) Change (relative to day 14) in left ventricular end-diastolic volume (LVEDV). (**E**) Changes in stroke volume at different time points. ANOVA with Bonferroni's post-hoc test was used for comparisons in **A**, **C**, **D**, and **E**. The Mann-Whitney test was used for comparisons in **B**. Data are presented as the mean±SEM. **P*<0.05, ***P*<0.01, ****P*<0.001.

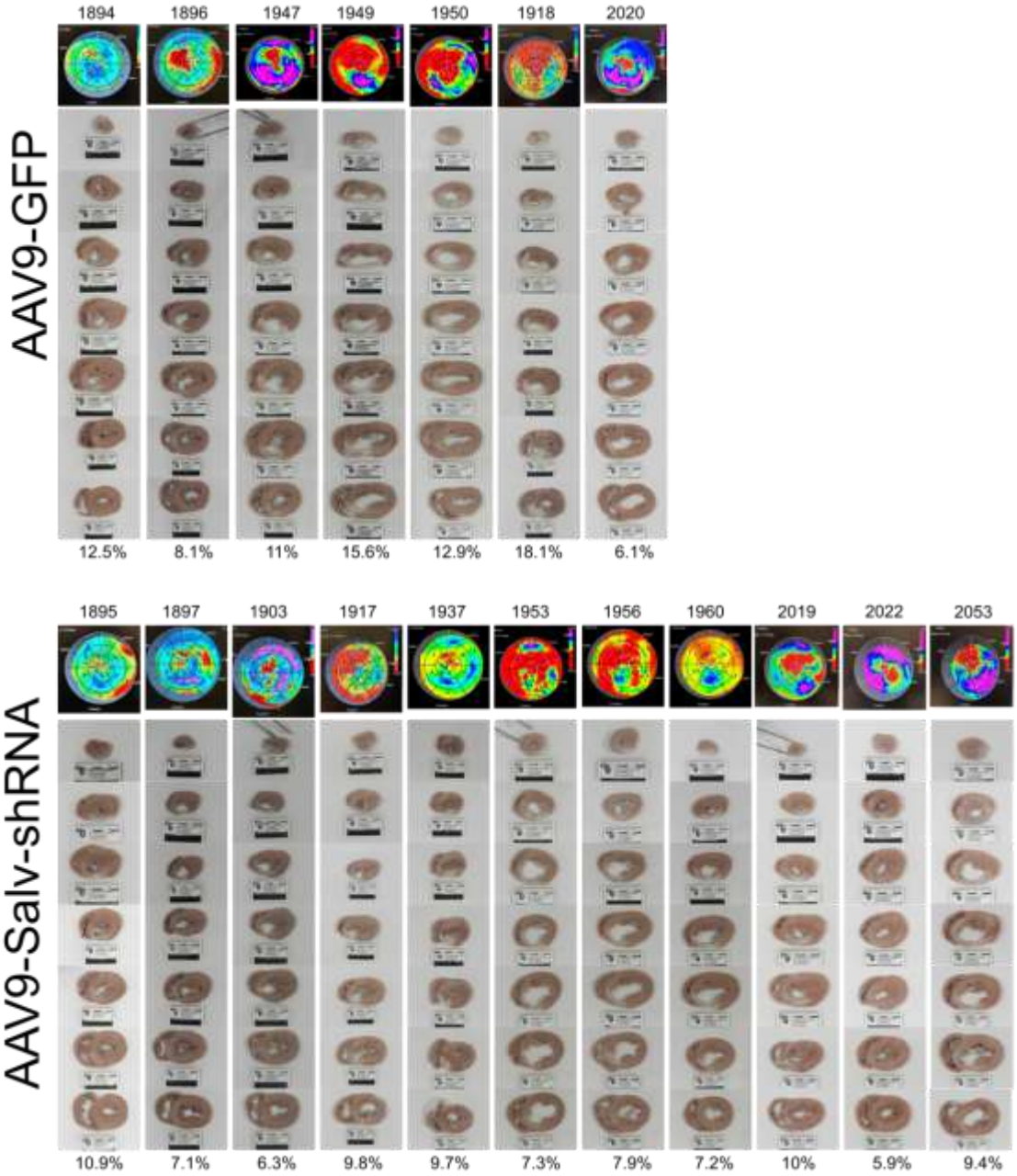

Fig. S6 Decreased cardiac scar sizes in *Sav* knockdown pigs. Summary of all slices from the hearts of pigs injected with AAV9-GFP (top) or AAV9-*Sav*-shRNA (bottom, low and high-dose combined). NOGA maps at the top of each column show the injection sites in each pig. Quantified scar areas are shown at the bottom of each column.

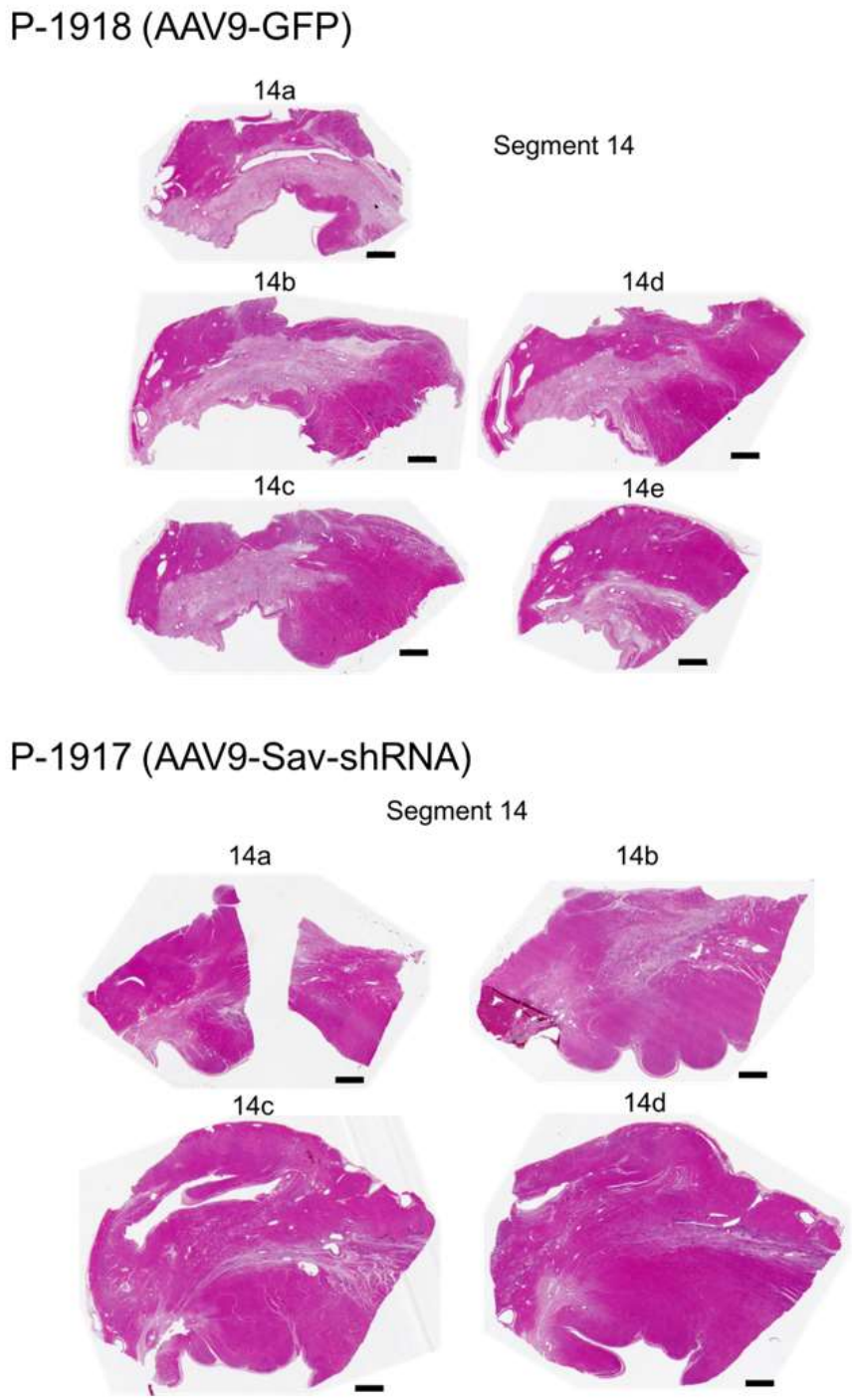

Fig. S7 Decreased cardiac fibrosis in *Sav* knockdown pigs. Hematoxylin and eosin–stained sections from pigs P-1917 (AAV9-*Sav*-shRNA low-dose) and P-1918 (AAV9-GFP). Sections are from similar areas in both pigs (segment 14).

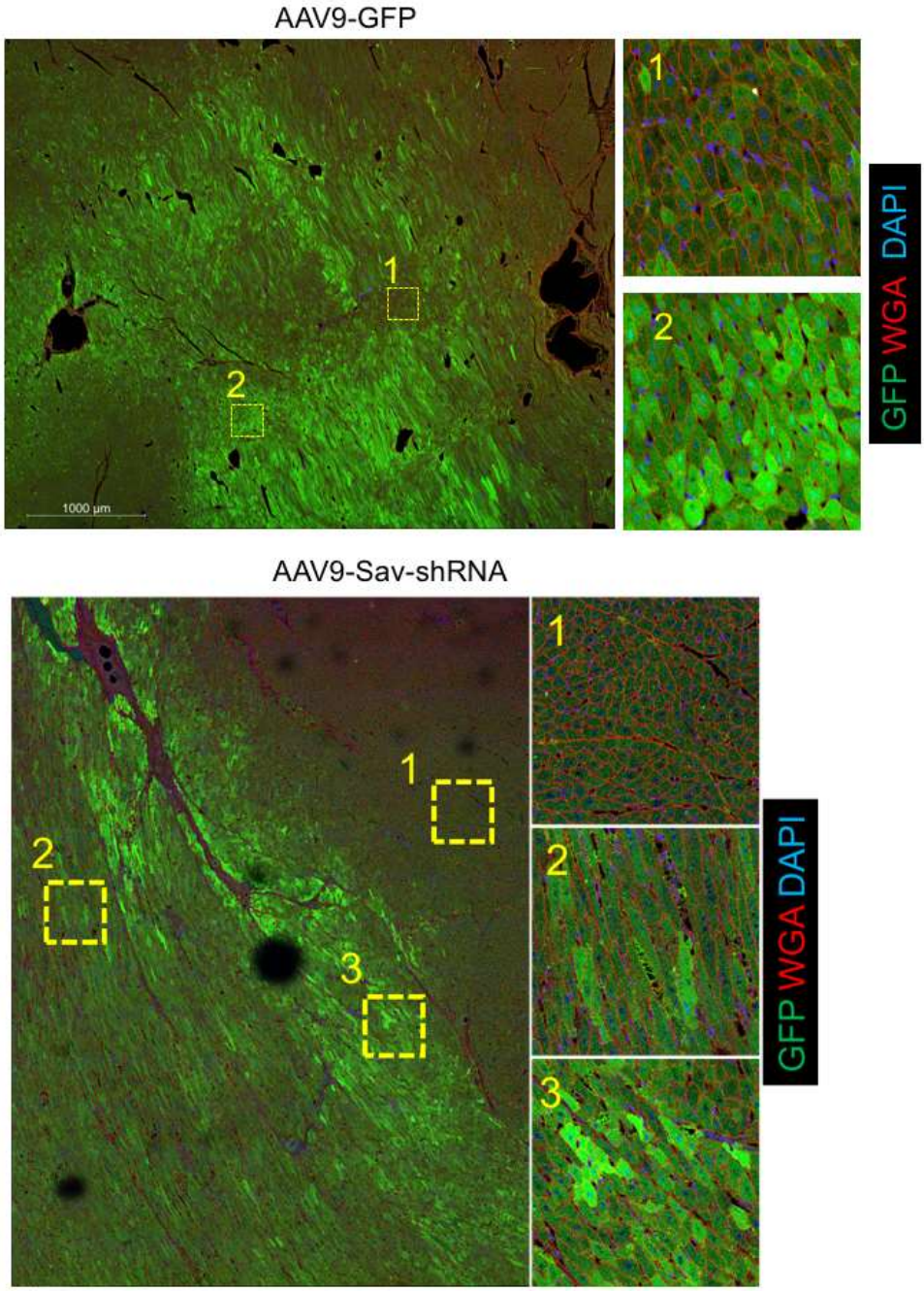

Fig. S8 AAV9 vector expression in pig hearts. Immunofluorescence staining showing GFP expression approximately 90 days after virus injection (AAV9-GFP, pig P-1950; AAV9-*Sav*-shRNA low-dose, pig P-1895).

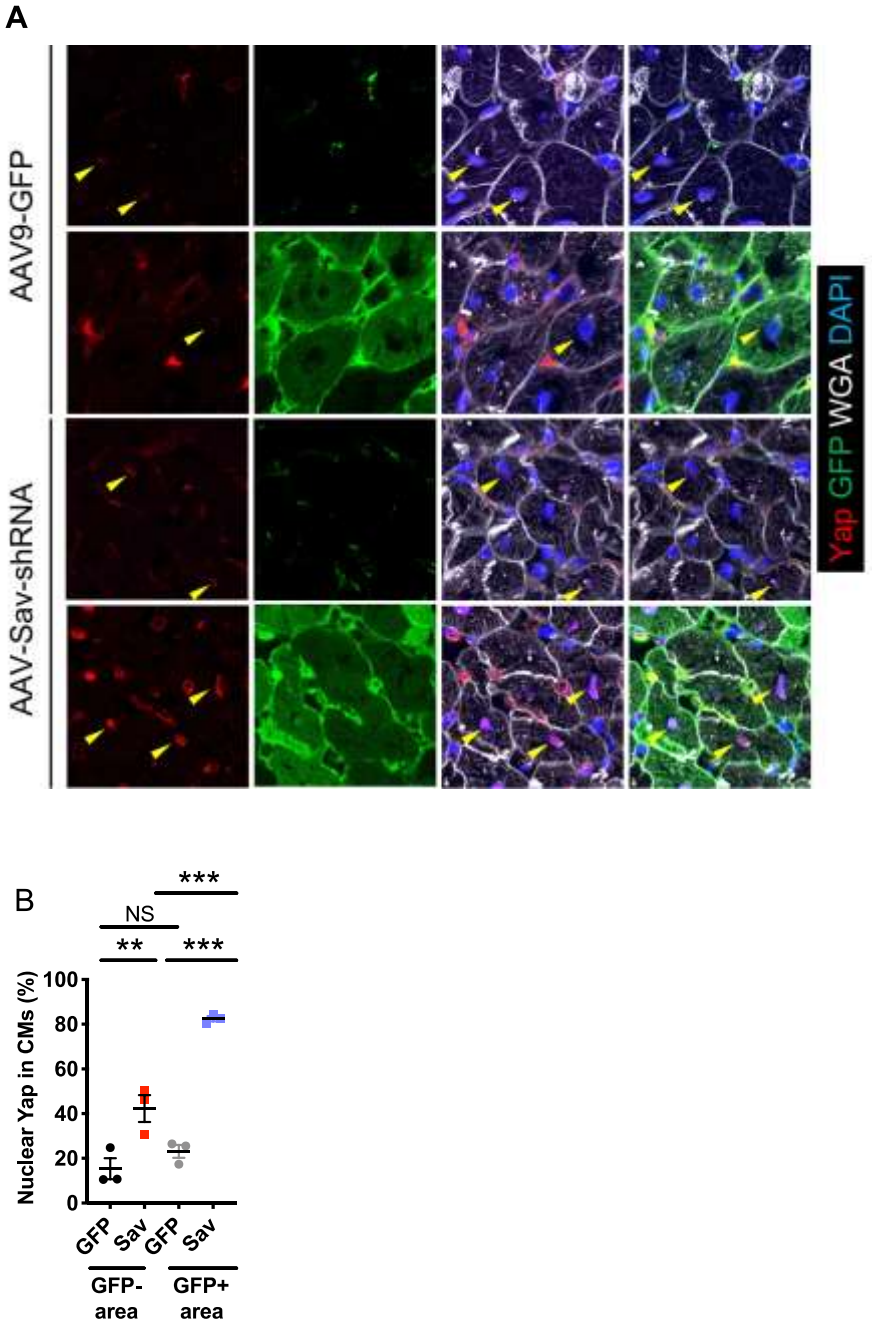

Fig. S9 Yap staining 3 months after viral injection. (**A**) Yap staining in pig hearts injected with AAV9-GFP (GFP) or AAV9-*Sav*-shRNA high-dose (Sav). (**B**) Quantification of nuclear Yap. One-way ANOVA with Tukey's post-hoc test was used for comparisons (n=3). Data are presented as the mean±SEM. ***P*<0.01, ****P*<0.001.

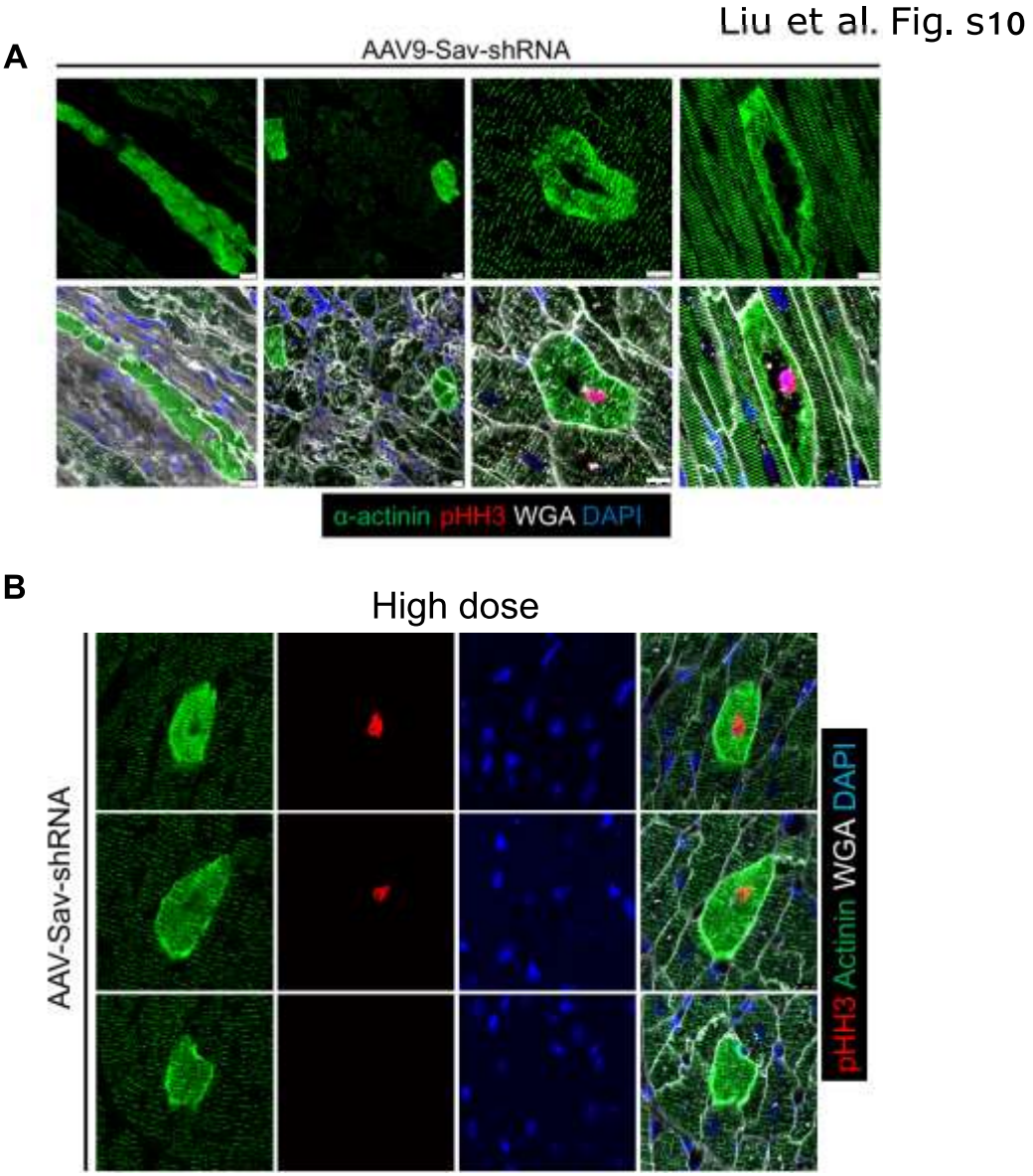

Fig. S10 Sarcomere breakdown in *Sav* knockdown cardiomyocytes. Immunofluorescence staining for pHH3 and sarcomere actinin in hearts which received low-dose (**A**) or high-dose of AAV9-*Sav*-shRNA (**B**).

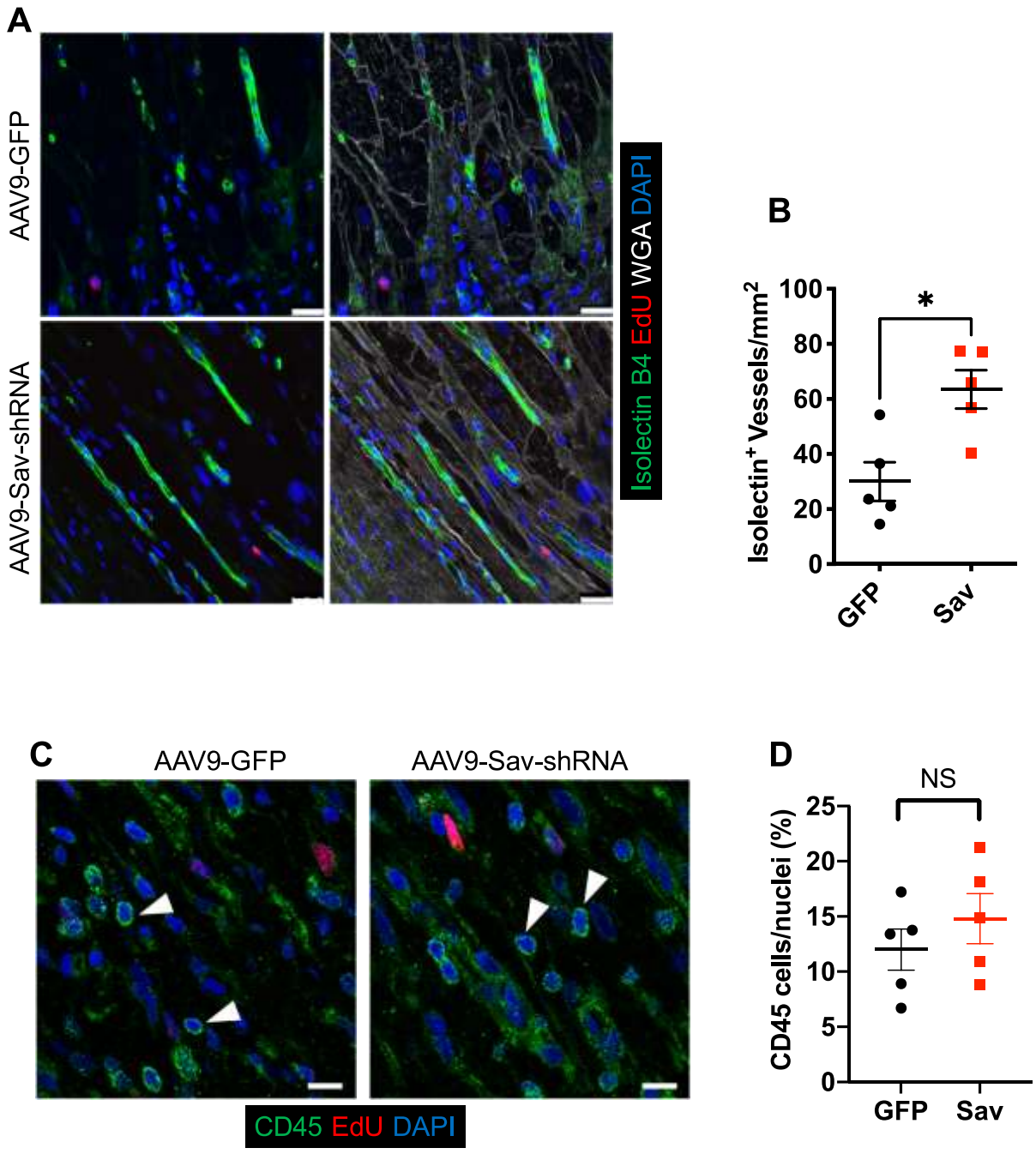

Fig. S11 Increased vascularity in *Sav* knockdown pigs. (**A**) Immunofluorescence staining for isolectin B4 reveals endothelial cells in the infarct tissue of pig hearts at 90 days after virus injection. Quantification of data is shown in (**B**). For each pig heart, 2 to

4 tile images were quantified (n=5). (**C**) Immunofluorescence staining for CD45 showing leukocytes in the infarcted tissue of pig hearts at 90 days after virus injection. Quantification of data is shown in **D**. For each pig, 5 images were quantified (n=5). GFP, AAV9-GFP; Sav, AAV9-Sav low-dose. The Mann-Whitney test was used for comparisons. Data are presented as the mean±SEM. *P<0.05.

Table S1. Pathology report for other organs

Animal ID	Lungs	Liver	Kidneys
P-1894	Dorsal caudal dark red discoloration, mild	Normal	Right renal hypoplasia
P-1895	Dorsal caudal dark red discoloration, mild/moderate	Normal	Normal
P-1896	Dorsal caudal dark red discoloration, minimal	Normal	Normal
P-1897	Small, focal reddening, minimal (left caudal lobe)	Normal	Normal
P-1903	Left lung: Dorsal caudal dark red discoloration, mild; caudal lobe collapse, moderate	Normal	Left kidney: 1 multilocular, 1 unilocular cyst, cranial pole
P-1917	Dorsal caudal dark red discoloration, minimal	Normal	Normal
P-1918	Dorsal caudal dark red discoloration, mild	Normal	Normal
P-1937	Dorsal caudal dark red discoloration, minimal	Gallbladder: Thin, darkened wall	Normal
P-1947	Dorsal caudal congestion,	Normal	Right kidney: 1

	patchy, mild; multiples of reddening		multilocular, 1 unilocular cyst, cranial pole
P-1949	Dorsal caudal dark red discoloration, mild	Normal	Normal
P-1950	Dorsal caudal dark red discoloration, mild; ventral extensive reddened areas, middle lobes	Normal	Normal
P-1953	Dorsal caudal dark red discoloration, mild	Normal	Normal
P-1956	Dorsal caudal dark red discoloration, mild/moderate	Normal	Normal
P-1960	Dorsal caudal dark red discoloration, mild	Normal	Normal
P-2019	Dorsal caudal dark red discoloration, minimal Pinpoint-sized (≤1 mm) black/brown specks, few/scattered, superficial and deeply located	Normal	Normal
P-2020	Dorsal caudal dark red discoloration, mild	Normal	Right kidney: 2 unilocular cysts, medullary

P-2022	Dorsal caudal dark red discoloration, mild	Normal	Left kidney: 1 unilocular cyst, medullary
P-2053	Dorsal caudal dark red discoloration, mild/moderate	Normal	Normal

Table S2. Microscopic evaluation of the lungs

Animal ID	Section	Description
P-1937	1-17	Lung (right, left, all lobes) - Areas of atelectasis, moderate, mostly in the caudal portions of the diaphragmatic lobes
P-1947	9	Lung (right middle lobe, mid) - Areas of atelectasis, moderate
	14	Lung (left cranial lobe, apical, mid) - Areas of atelectasis, moderate
P-1949	32	Lung (right middle lobe, mid) - Normal
	39	Lung (left cranial lobe, caudal) - Normal
P-1950	37	Lung (right middle lobe, cranial, mid) - Interstitial pneumonia, focal. Thickening and consolidation of alveolar septae; mild focal increase in BALT, with reactive follicles; neutrophilic presence in some areas; few clusters of multinucleated giant cells
	42	Lung (left cranial lobe, cranial, mid) - Interstitial pneumonia, focal. Thickening and consolidation of alveolar septae, with chronic inflammatory cells and some areas of neutrophilic presence; focal multinucleated giant cells in some areas, sparingly with presence of foreign material
P-1953	41	Lung (right middle lobe, mid) - Normal
	48	Lung (left cranial lobe, caudal) - Normal
P-1956	21	Lung (right middle lobe, mid) - Normal
	26	Lung (left cranial lobe, cranial, mid) - Normal
P-1960	21	Lung (right middle lobe, cranial, mid) - Normal
	28	Lung (left cranial lobe, caudal) - Normal

	36	Lung (left cranial lobe, cranial, mid) - Mild lymphocytic inflammation surrounding the airways

Table S3. Microscopic evaluation of the liver

Animal ID	Section	Description
P-1937	42	Liver (right lateral lobe, mid) - Normal
	45	Liver (right medial lobe, mid) - Normal
	48	Liver (left medial lobe, mid) - Normal
	51	Liver (left lateral lobe, mid) - Normal
P-1947	21	Liver (right lateral lobe, mid) - Normal
	24	Liver (right medial lobe, mid) - Normal
	27	Liver (left medial lobe, mid) - Normal
	30	Liver (left lateral lobe, mid) - Normal
P-1949	46	Liver (right lateral lobe, mid) - Normal
	49	Liver (right medial lobe, mid) - Normal
	52	Liver (left medial lobe, mid) - Normal
	55	Liver (left lateral lobe, mid) - Normal
P-1950	22	Liver (right lateral lobe, mid) - Normal
	25	Liver (right medial lobe, mid) - Normal
	28	Liver (left medial lobe, mid) - Normal
	31	Liver (left lateral lobe, mid) - Normal
P-1953	24	Liver (right lateral lobe, mid) - Normal
	27	Liver (right medial lobe, mid) - Normal
	30	Liver (left medial lobe, mid) - Normal
	33	Liver (left lateral lobe, mid) - Normal

P-1956	33	Liver (right lateral lobe, mid) - Normal
	36	Liver (right medial lobe, mid) - Normal
	39	Liver (left medial lobe, mid) - Normal
	42	Liver (left lateral lobe, mid) - Normal
P-1960	41	Liver (right lateral lobe, mid) - Normal
	44	Liver (right medial lobe, mid) - Normal
	47	Liver (right lateral lobe, mid) - Inflammation, focal, minimal. Single focus (~ 300 μm diameter) of chronic inflammatory cell infiltrate, not grossly apparent
	50	Liver (left lateral lobe, mid) - Normal

Table S4. Overall Inflammation Grade in Injected and Non-Injected Heart sections

Animal ID	Inflammation Grade	
	Injected Segments	Non-Injected Segments
P-1894	Mild	None
P-1895	Moderate	None
P-1896	Minimal	None
P-1897	Mild	None
P-1903	Mild	None
P-1917	Moderate	Minimal
P-1918	Moderate	Minimal
P-1937	None	None
P-1947	None	None
P-1949	Minimal	None
P-1950	Minimal	Minimal
P-1953	Minimal	None
P-1956	None	None
P-1960	Mild	Minimal
P-2019	Mild	None
P-2020	Mild	None
P-2022	None	None
P-2053	Moderate	None

Table S5. Incidence of inflammation by NOGA sections

Animal ID	Injected Segments			Non-Injected Segments		NOGA Injection Pattern
	NOGA Segment	# Injections	Affected Sections	NOGA Segment	Affected Sections	
P-1894	7	1	1/4	5	0/1	Dispersed
	8	2	1/4			
P-1895	13	2	1/6	5	0/1	Dispersed
	14	2	5/5			
P-1896	15	1	2/6	5	0/1	Dispersed
	16	1	1/6			
	7	1	0/5			
P-1897	14	1	0/5	5	0/1	Dispersed
	15	2	1/4			
	8	2	2/5			
P-1903	7	2	0/4	5	0/1	Dispersed
	8	2	1/4			
	14	2	3/5			
P-1917	17	1	2/2	2	0/1	Dispersed
	14	3	4/4	3	1/1	
	9	4	5/5	13	0/1	
P-1918	14	2	4/5	5	1/1	Dispersed
	6	4	5/6	4	1/1	

				13	1/1	
P-1937	17	3	0/4	13	0/1	Clustered
	14	4	0/5	6	0/1	
	15	2	0/5	5	0/1	
P-1947	16	3	0/4	13	0/1	Clustered
	12	2.5	0/5	10	0/1	
	6	2	0/2	3	0/1	
P-1949	15	2.5	0/5	13	0/1	Clustered
	9	2	1/4	3	0/1	
	4	4	0/4	6	0/1	
P-1950	12	4.5	0/6	4	1/1	Clustered
	9	5	2/5	5	0/1	
				13	0/1	
P-1953	4	2	1/2	6	0/1	Clustered
	15	2	1/3	3	0/1	
	10	6	3/8	7	0/1	
P-1956	16	1.5	1/6	13	0/1	Clustered
	11	6	0/4	6	0/1	
	5	3	0/2	4	0/1	
	7	2	0/2			
P-1960	5	2	3/3	1	1/1	Clustered
	11	3	3/6	4	1/1	

	9	4	3/5	13	1/1	
P-2019	16	2	3/3	6	0/1	Clustered
	14	2	2/3	13	0/1	
	12	2	0/3			
P-2020	16	1	2/2	4	0/1	Clustered
	13	1	0/1			
	12	3	2/4			
	8	3	0/4			
P-2022	6	3	0/3	4	0/1	Clustered
	12	4	0/2	3	0/1	
	7	1	0/2			
	13	3	0/1			
	14	2	0/2			
P-2053	14	2	4/4	1	0/1	Clustered
	15	2	4/4	13	0/1	
	16	1	1/4	7	0/1	
	11	4	4/4			
	9	5	5/5			

Table S6. Body weight for pigs

Body weights

Viral injection	ID number	before-MI	2 weeks after MI	10 days after virus	20 days after virus	30 days after virus	40 days after virus	50 days after virus	60 days after virus	80 days after virus	90 days after virus
AAV9-GFP	P-1894	33.11	36.6	40.7	43.9	43.6	47	48.2	45.81		
	P-1896	26.3	31.8	35.2	35.5	38	39	40.5	42.7	43.09	45.81
	P-1918	28.57	33	33.2	33.9	36.4	38.6	41.27	42.63	47.4	50.12
	P-1947	23.1	28	31.4	30.9	34.5	35.7	36.1	37.3	38.1	40.3
	P-1949	26.76	31.8	34.1	35.5	38.6	38.6	39.91	40.82	43.99	45.8
	P-1950	26.76	30.8	32	33.2	33.9	34.01	34.1	35.15	35.38	37.19
	P-2020	28.6	29.5	30.9	33.2	37	39	40	40.2	47.7	49.5
AAV9-Sav-shRNA	P-1895	34.01	38.6	41.4	44.5	46.1	44.3	44.8	46.8		
	P-1897	29.02	34.8	38.2	38	41.4	42.3	43	44.8	45.81	49.21
	P-1903	25.4	28.6	32.5	32.7	33.9	35.5	36.1	37	40	42.86
	P-1917	30.39	34.5	36.8	40.5	37.7	41.3	42	43.54	46.72	48.98
	P-1937	26.76	31.8	33.6	38	38.4	37	40.5	40	43.5	43.54
	P-1953	25.85	30	30.5	30.7	34.3	36.4	34.92	37.42	37.19	38.55
	P-1956	26.7	31.4	34.1	35.9	35.9	36.8	37.5	40	40.8	43
	P-1960	24.04	28.2	28.2	29.3	30.7	31.4	33.11	33.11	37.64	38.55
	P-2019	38.6	38.6	39.5	41.6	43.6	44.1	44.1	43.9	49.5	53

	P-2022	30.5	31	35.9	37.3	38.2	39	39.5	41.6	46.8	52.3
	P-2053	34	36	38	40	42.7	46	49.1	52	61	64
	P-2066	33	36	38	40	45					
	P-2067	35	37.7	41	41	41					
	P-2069	26	26.5	27.5	29	30					
	P-2070	26	27	27	29	30					
	P-2071	27	27.5	27.5	30	31					
	P-2073	25	27	27.5	27.7	29					
	P-2075	28	29.5	30	32	32					